

## Review



**Cite this article:** Whyte D. 2019 Small, modular and economically attractive fusion enabled by high temperature superconductors. *Phil. Trans. R. Soc. A* **377**: 20180354.  
<http://dx.doi.org/10.1098/rsta.2018.0354>

Accepted: 3 December 2018

One contribution of 14 to a discussion meeting issue 'Fusion energy using tokamaks: can development be accelerated?'

### Subject Areas:

plasma physics, nuclear physics

### Keywords:

fusion energy, tokamaks, superconductors

### Author for correspondence:

Dennis Whyte

e-mail: [whyte@psfc.mit.edu](mailto:whyte@psfc.mit.edu)

<sup>†</sup>The present paper was initially written by Jack Connor and Colin Windsor from the audio transcript and slides of the presentation, before being edited by the author.

# Small, modular and economically attractive fusion enabled by high temperature superconductors

Dennis Whyte<sup>†</sup>

MIT Plasma Science and Fusion Center, 77 Massachusetts Avenue, 24-107, Cambridge, MA 02139, USA

The advantages of high magnetic fields in tokamaks are reviewed, and why they are important in leading to more compact tokamaks. A brief explanation is given of what limits the magnetic field in a tokamak, and why high temperature superconductors (HTSs) are a game changer, not just because of their higher magnetic fields but also for reasons of higher current density and higher operating temperatures. An accelerated pathway to fusion energy is described, defined by the SPARC and ARC tokamak designs.

This article is part of a discussion meeting issue 'Fusion energy using tokamaks: can development be accelerated?'

## 1. Introduction

The left-hand part of figure 1 shows the structure of a tokamak with its yellow plasma forming a torus. Its key parameters are its major radius  $R$ , and the magnetic field  $B$ , which the blue coils create along the toroidal (long-way round) plasma path. Why are we talking about tokamaks? The answer lies to the right of figure 1, which shows the approach to the Lawson fusion criterion for net energy in terms of the product of energy confinement time and density versus the temperature. The blue points are tokamaks, and green is everything else. The tokamaks have much the highest products. That's why we are talking about tokamaks if we want an accelerated path to fusion.

The most pressing need for the development of an economically attractive fusion power plant is to achieve the required nuclear physics and absolute confinement

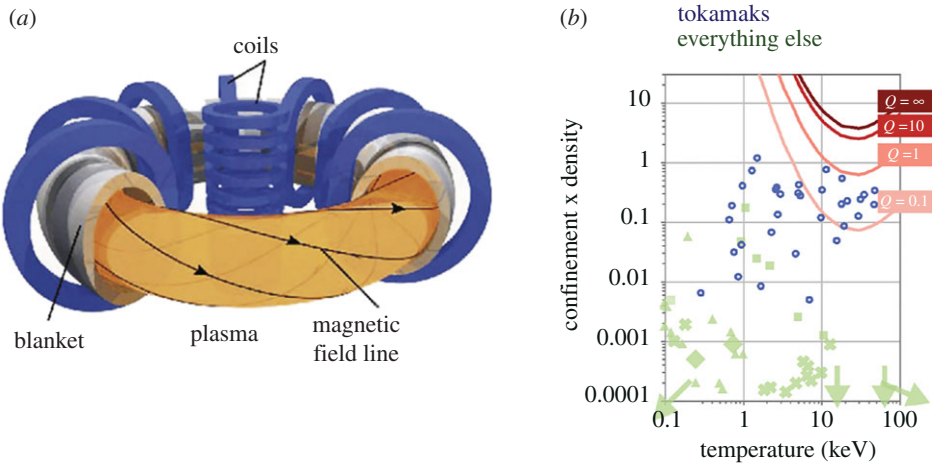


**Figure 1.** (a) The structure of a tokamak (courtesy of Yuhong Xu [1]). (b) The approach to the Lawson fusion criteria showing the product of the energy confinement time times the density against the temperature. The blue tokamaks are closer to the right-hand upper corner than the green symbols of other configurations (courtesy of Daniel Brunner). (Online version in colour).

parameters, rather than size,  $R$ , magnetic field strength,  $B$ , plasma beta,  $\beta$  or safety factor,  $q$ , for example, which appear nowhere in the Lawson criterion. One can distinguish two objectives on the path: (i) a Science Mission that achieves a self-heating burning plasma requiring plasma parameters such that  $p_{\text{th}}\tau_E = 1 \text{ MPa s}$ , where  $p_{\text{th}}$  is the thermal plasma pressure and  $\tau_E$  is the energy confinement time, and ion and electron temperatures  $T_i$  and  $T_e$ , such that  $T_i \approx T_e \sim 10\text{--}20 \text{ keV}$ , and (ii) an Energy Mission, requiring an energy gain and a volumetric fusion power density,  $P_{\text{fus}} \text{ (MW m}^{-3}\text{)} \approx 8p_{\text{th}}^2 \text{ (MPa)}$ .  $B$  and  $R$  are the two fundamental design parameters in achieving these missions. The cost of a tokamak, the most promising confinement device, including the vacuum chamber and the blanket, is roughly proportional to the volume,  $V \sim R^3$ , while achieving the requisite performance for  $p_{\text{th}}\tau_E$  in the Lawson diagram requires sufficient energy confinement, and thermal pressure, gained by the confining and stabilizing magnetic field  $B$ .

In the following section, we will demonstrate the impact of  $B$  and  $R$  on the relevant physics for these missions in more detail. It proves desirable to maximize  $B$ , but we will discuss the technical limits to this. A discussion follows on how the advent of high temperature superconductors (HTS) is a ‘Game changer’, allowing the possibility of much greater magnetic fields in compact devices. Finally, an accelerated pathway to fusion energy, underway at MIT with funding from Commonwealth Fusion Systems (CFS), is described that takes advantage of these developments. It involves a burning plasma demonstration device, SPARC, that would produce a ‘Kitty Hawk moment’, to be followed by a commercial power station to produce fusion energy, ARC. Some brief conclusions are given.

## 2. The role of magnetic field and size and their limits

From the economic point of view, the volumetric fusion power density is a strong function of  $B$ . The plasma beta,  $\beta$ , measures the efficiency of the magnetic field in containing plasma pressure:  $\beta = p_{\text{th}}/p_{\text{mag}} = p_{\text{th}}/(B^2/2\mu_0)$ . However,  $\beta$  is limited by the Troyon criterion for plasma stability:  $\beta_N = \beta q/5\varepsilon S(\kappa)$ ; here  $\varepsilon$  is the inverse aspect ratio of the tokamak and  $S(\kappa)$  is a shape factor dependent on plasma elongation,  $\kappa$ . Since,  $P_{\text{fus}} \approx 8p_{\text{th}}^2$ , this implies  $P_{\text{fus}} \sim (\beta_N^2 \varepsilon^2 S q^2) B^4$ . The energy gain,  $Q$ , depends on the confinement quality. One anticipates that plasma energy loss is by diffusion:  $\tau_E \sim a^2/D$ , with  $D \sim (a/\rho)^2$ , where the Larmor radius,  $\rho \sim 1/B$ , so  $\tau_E \sim B^2$ , although this dependence is substantially more complicated in reality by turbulent heat transport. A further

**Table 1.** The variation of several tokamak issues of importance with magnetic field  $B$  and tokamak major radius  $R$ .

issue	scaling	issue	scaling
power density	$B^4$	density (tokamak)	$R^{-1}B^1$
confinement (generic)	$R^2B^2$	density (stellarator)	$\beta B^{2.5}$ (burning)
confinement (tokamak)	$R^{2.7}B^{3.5}$ ( $H_{98}$ )	heat exhaust: min. $f_z$	$B^{-1}$ (burning)
	$R^{3.1}B^{2.1}$ (Petty)	runaway e-amp	$\exp(R^{0.28})/B^{0.3}$
confinement (stellarator)	$R^{2.8}B^{2.1}$	synchrotron: runaways	$B^2$
gain	$R^{2-3.1}B^{4-5.5}$	synchrotron: thermal	$\sim B^{1.5}$
stable pedestal/I-mode	$\sim \beta_N B^2$	TAE	$n \sim B, Va \sim B$

**Table 2.** The variation of key tokamak parameters as the safety factor  $q$  and field  $B$  are varied by factors of 2.

	scenario	(i)	(ii)	(iii)
	ITER	$q \times 2$	$B \times 2 R/2$	$B \times 2 R/2 q \times 2$
$B$ (T)	5.3	5.3	10.6	10.6
$R$ (m)	6.2	6.2	3.1	3.1
$V$ (m <sup>3</sup> )	890	890	111.25	111.25
$q/3$ safety factor	1	2	1	2
$n_{20}$ (m <sup>-3</sup> )	1	0.5	4	2
$T$ (keV)	9	5.3	12	10.6
$P_{\text{fus}}$ (MW)	500	44	1800	714
$Q$	10	0.9	36	14
$P_f/V$ (MW m <sup>-3</sup> )	0.6	0.05	16	6.5

consideration for a tokamak is the empirical Greenwald limit on the density,  $n < n_G = I_p/a^2 \sim S(\kappa) B/qR$ , where  $I_p$  is the plasma current. Then,  $P_{\text{fus}} \sim n^2 \sim B^2/R^2$ , which indicates the Greenwald limit, actually punishes large size.

An APS Review in 2017 [2] found the advantages of high  $B$  spanned a huge range of physics issues, as shown in table 1, where various empirical confinement scalings are used. It is instructive to play a ‘double and half design game’, which takes ITER parameters and considers three scenarios: (i) double safety factor  $q$ ; (ii) double the field  $B$  and half the size  $R$ ; and (iii) double  $B$ , half  $R$  and double  $q$ . Table 2 shows the impacts on  $P_{\text{fus}}$ , the energy gain parameter,  $Q$  and  $P_{\text{fus}}/V$ . In scenario (ii), one achieves an improvement in  $P_{\text{fus}}/V$  by a factor 27, which even exceeds a scaling like  $B^4$ ! The attractiveness of scenario (ii) arises from a combination of both high  $B$  and small size  $R$ . Confinement is little affected because the product  $B R$  remains the same as in ITER which means that the same number of gyro-radii are contained, but the density limit allows the quadrupling of density, which at the same  $T$  provides a 16-fold increase in fusion power density. There is basically no scenario where higher  $B$  is detrimental [3].

This all raises the issue of what limits the magnitude of  $B$  in a tokamak and the physics of the coils to provide it. It is interesting to realize that an electromagnet and a tokamak plasma obey the same physics: Ampere’s law, force balance and ohmic heating. Ampere’s law implies  $B \sim j$ , the current density, while the latter two imply  $p_{\text{mag}} \sim B^2$ . However, they involve different media, and this strongly affects the resistivity appearing in the ohmic heating condition. A DT plasma operates at up to  $T \sim 10^8$  K, whereas a Cu coil may be at 10–100 K and a superconducting coil at less than 10 K.

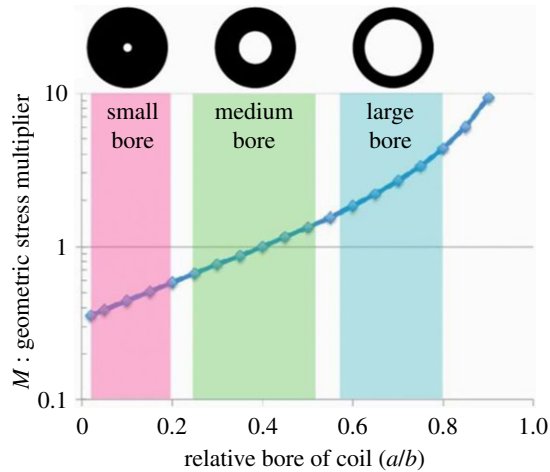


**Figure 2.** The variation of stress in a coil plotted against the relative bore of a coil. The geometric factor  $M$  favours small bore magnets. (Online version in colour.)

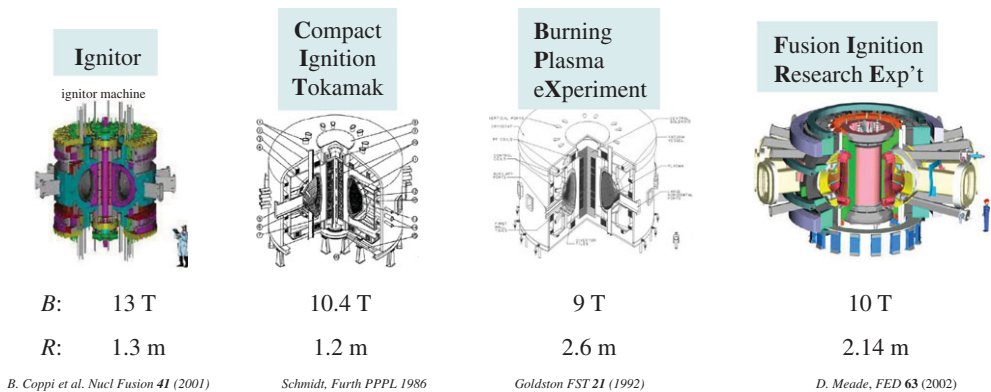


**Figure 3.** Tokamaks with cryogenic copper coils produce pulsed, high gain burning plasmas at very modest size, with magnetic fields on the plasma of order 10 T. (Online version in colour.)

As in toroidal plasma physics, aspect ratio is a critical and complex optimization matter. For a coil, one can characterize the bore by  $x = a/b$ , where  $a$  is the radius of the bore and  $b$  that of the coil, distinguishing small bore,  $x < 0.2$ , medium bore,  $0.3 < x < 0.5$  and large bore,  $0.6 < x < 0.8$ , as in figure 2. The stress on the coils can be expressed as  $\sigma = MB^2/2\mu_0$ , where the generic stress multiplier  $M = (2x + 1)/(3 - 3x)$ , thus favouring small bores. However, fusion requires large bore size because that is where the plasma and blanket must be located. Another limitation in toroids is that the coil geometry makes the maximum field, and stresses, about twice as large on the inside part of the torus, but it is the  $B$  field at the plasma that sets its performance.

The high-field tokamak Alcator used coils made from a combination of Cu sandwiched between stainless steel immersed in liquid N at 70 K, enabling an axial field  $B_0 \sim 11$  T and  $B_{\max} \sim 22$  T. In operation, the Cu resistance doubled in 10 s. With cryogenic Cu magnets, one can access  $B_{\text{coil}} > 20$  T and  $B_0 \sim 10$  T for a pulsed, high gain burning plasma at very modest size. Figure 3 shows parameters for several such tokamaks: Ignitor [3], CIT [4], BPX [5] and FIRE [6].

The ITER device uses low temperature superconductor (LTS) coils, but these have a restricted operating space in  $T$ ,  $j$  and  $B$ , as shown in figure 4. The critical value of  $j$ , at fixed operating  $T$ , depends on the type of superconductor and on  $B$ . One can characterize the critical value of  $j$  by

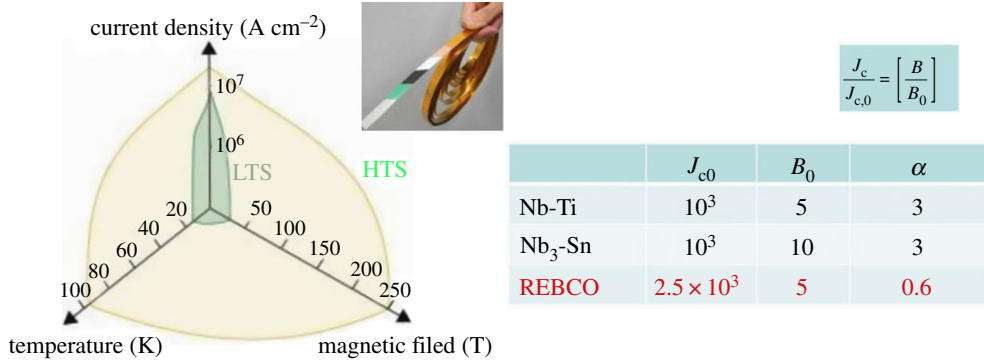


**Figure 4.** The space covered in temperature, current density and magnetic field by conventional LTS and by HTSs. (Online version in colour.)

$j_{\text{crit}}/j_{\text{crit}0} = (B/B_0)^\alpha$ , where the parameters  $j_{\text{crit}0}$  and  $\alpha$  are given for Nb-Ti and Nb<sub>3</sub>-Sn for  $T \sim 4$  K in the inset table in figure 4. Thus, the magnetic field from an Nb-based superconducting coil at  $T \sim 4$  K, consisting of stainless steel surrounding superconductor strands immersed in a Cu coil channel surrounding, in turn, a coolant channel, is limited to approximately 8 T for Nb-Ti and 13 T for Nb<sub>3</sub>-Sn.

A US National Academy report [7] found that a cryogenic Cu-based tokamak, FIRE, could study burning plasma science at a volume 25 times smaller than one based on Nb<sub>3</sub>-Sn, because  $p_{\text{th}}\tau_E \sim R^{2.7}B^{5.5}$ ,  $V \sim R^3 \sim 1/B^5$ . High  $B$  compact devices were known to have 10 times the performance to cost ratio around 1996, but they were pulsed machines; thus, the emphasis was on extrapolating lower- $B$  devices to long pulse. However, the advent of HTS is a game changer.

### 3. High temperature superconductors

The operating range of new HTSs, which are commercially available, is much greater. Figure 4 also showed how the REBCO HTS extends the range of  $j$  and  $B$ , with the inset table in figure 4 also showing its parameters  $j_{\text{crit}0}$ ,  $B_0$  and  $\alpha$ . With HTS magnets, the only limiting factor is stress and multiple design choices are available to achieve  $B_0 > 10$  T. Figure 5 inset shows the design of a coil in which stainless steel surrounds a copper wire in which HTS tapes are immersed, with coolant flowing through its bore. The critical current and the maximum stress,  $\sigma_{\text{max}}$ , as functions of  $B_{\text{max}}$ , are also shown in figure 5; the latter depends on the proportion of stainless steel in the coil. The size of the bore is a key parameter for determining stress and small bore magnets with  $B > 40$  T have already been demonstrated in the field of NMR. The availability of HTS magnets clearly changes the landscape for magnetic confinement fusion. It means that it becomes possible to extrapolate high-field designs like Ignitor and CIT to long pulse devices.

### 4. An accelerated pathway to fusion energy

A new strategy for speeding the development of fusion energy is being pursued at MIT with private sector funding from CFS. It is based on using HTS magnets in compact, high-field tokamak devices. Phase 1 builds on the C-Mod tokamak with work on HTS magnets (cost  $\sim$  \$80 M) in progress. Phase 2 is to build SPARC, a prototype demonstration device to produce a burning plasma, followed by ARC, a demonstration commercial power plant.

SPARC could be considered as the ‘Kitty Hawk’ moment for fusion. Its size is set by the confinement required to produce net energy:  $Q > 2$  and  $P_{\text{fus}} > 50$  MW. The SPARC device is shown in figure 6. Its parameters are:  $B = 12$  T,  $P_{\text{fus}}$ : 50–100 MW,  $Q > 2$ ,  $V \sim 11$  m<sup>3</sup>, 10 s pulse-length, allowing plasma  $j$  to be in equilibrium and a low neutron fluence (1/500th of that in ITER).



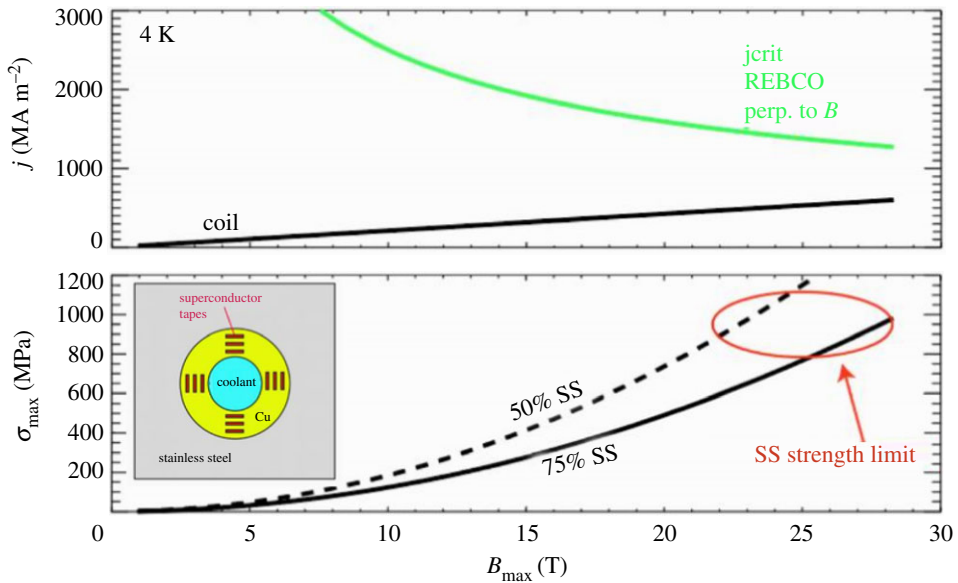


**Figure 5.** Stress, rather than the critical current capacity, becomes the limiting factor of the fields obtainable with HTS magnets. However, there are multiple design routes available to reach fields of order 10 T at the plasma. (Online version in colour.)

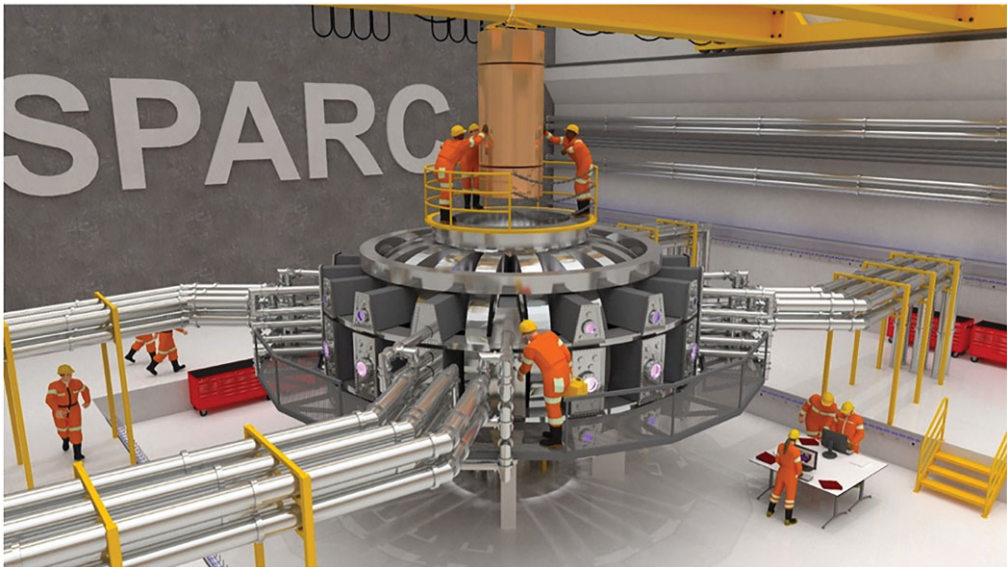


**Figure 6.** The SPARC project could be the ‘Kitty Hawk’ moment of fusion, giving fusion energy gain in a compact design using HTS magnets. (Online version in colour.)

ARC, on the other hand, requires producing sufficient DT neutrons to yield  $Q > 10$  and  $P_{\text{fus}} \sim 200$  MW. Figure 7 shows where these devices sit relative to ITER on a ‘size–magnetic field’ diagram, which is plotted for a fixed aspect ratio,  $A$ ,  $q$  and confinement  $H$ -factor,  $H = 1$ . It is striking to consider that the relative volumes concerned are: 880 : 140 : 12.

The concept of compact high-field, modular power (200 MW) devices that are possible with HTS enables further innovation. Thus, one can develop dismantlable coils, as on the right of

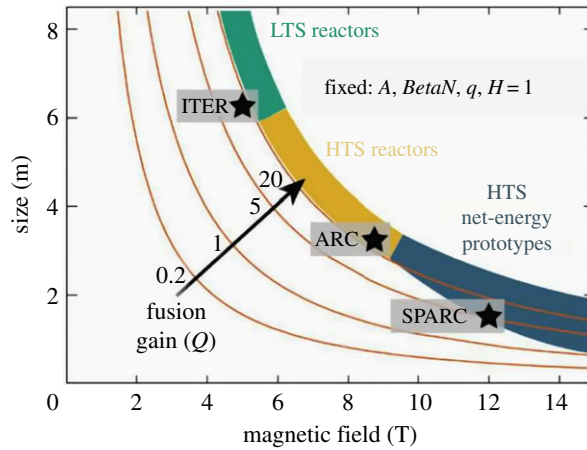


**Figure 7.** The new strategy to achieve fusion energy using HTS magnets. The tokamak size is plotted against the crucial parameter of magnetic field showing the three areas of low temperature superconductors (LTS), HTS reactors and HTS net-energy prototypes. (Online version in colour.)

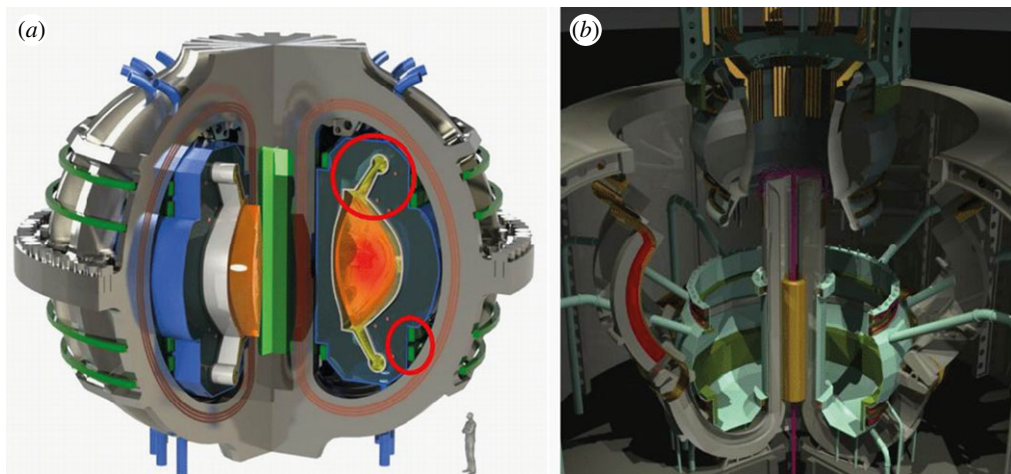


**Figure 8.** (a) The ARC project with its advanced high surface area divertor using internal HTS coils. (b) The de-mountable coil structure allowing a modular construction. (Online version in colour.)

figure 8, and advanced high surface area divertors using HTS coils, as to the left of figure 8 [8]. For the blanket, one can use liquid immersion FLiBe, which would have no damage limit, no gaps, volumetric heat removal and efficient tritium breeding.

## 5. Conclusion

Such compact devices would allow more rapid development and less risky access to private sector funding and offer the promise of the earlier realization of commercial fusion energy.

**Data accessibility.** This article has no additional data.

**Competing interests.** I declare I have no competing interests.

**Funding.** I received no funding for this study.

## References

1. Xu Y. 2016 A general comparison between tokamak and stellarator plasmas. *Matter and Radiation at Extremes* **1**, 192–200. (doi:10.1016/j.mre.2016.07.001)
2. Whyte D. 2017 The case for high field fusion, American Physical Society APS/DPP/2017. [http://firefusionpower.org/Whyte\\_FPA\\_2017.pdf](http://firefusionpower.org/Whyte_FPA_2017.pdf)
3. Coppi B, Airoldi A, Bombarda F, Cenacchi G, Detragiache P, Sugiyama LE. 2001 Optimal regimes for ignition and the Ignitor experiment. *Nucl. Fusion* **41**, 1253–1257.
4. Schmidt J *et al.* 1987 A compact ignition experiment, in plasma physics and controlled nuclear fusion research. In Proc. 11th Int. Conf., Kyoto, 13–20 November 1986, vol. III, p. 259, Vienna: IAEA.
5. Goldston RJ. 1992 Burning plasma experiment physics design. *Fusion Sci. Technol.* **21**, 1050–1055. (doi:10.13182/FST92-A29891)
6. Meade DM. 2002 FIRE, a next step option for magnetic fusion. *Fusion Eng. Des.* **63**, 531–540.
7. National Academies of Sciences, Engineering, and Medicine. 2018 Interim Report of the Committee on a Strategic Plan for U.S. Burning Plasma Research, [http://sites.nationalacademies.org/BPA/BPA\\_177107](http://sites.nationalacademies.org/BPA/BPA_177107), Burning Plasma—Bring a Star to Earth, September 2004. Final Report of the Burning Plasma Science Assessment Committee 2002–2004 National Academies of Sciences, Engineering, and Medicine.
8. Kuang AQ *et al.* 2018 Conceptual design study for heat exhaust management in the ARC fusion pilot plant. *Fusion Eng. Des.* **137**, 221–242.